ACADEMIA ROMÂNĂ
Revue Roumaine de Chimie
http://web.icf.ro/rrch/

Rev. Roum. Chim.,
2018, *63*(5-6), 425-435

Dedicated to Dr. Maria Zaharescu
on the occasion of her 80th anniversary

Sr DOPED Cu_2O A NEW p-TYPE MATERIAL FOR PHOTOVOLTAIC APPLICATIONS**

Mihai STOICA,[a] Mihai ANASTASESCU,[a*] Jose M. CALDERON-MORENO,[a] Madalina NICOLESCU,[a*] Petre OSICEANU,[a] Silviu PREDA,[a] Maria COVEI (DUTA),[b] Mircea MODREANU[c] and Mariuca GARTNER[a]

[a]"Ilie Murgulescu" Institute of Physical Chemistry of the Roumanian Academy, 202 Spl. Independentei, 060021 Bucharest, Roumania
[b] R&D Center Renewable Energy System and Recycling, Transilvania University of Brasov, Eroilor 29 Street, 500036, Brasov, Roumania
[c]Tyndall National Institute, University College Cork, Lee Maltings Complex, Dyke Parade, T12R5CP Cork, Ireland

Received July 24, 2017

A new class of transparent conductive oxides, namely Sr doped Cu_2O (Cu_2O-Sr) thin films, have been deposited by Metal Organic Chemical Vapor Deposition (MOCVD) method on glass substrate with 3:1 and 1:1 Sr:Cu molar ratios. The Cu_2O-Sr samples were investigated related to structure (X-Ray Diffraction, and Raman Spectroscopy), morphology (AFM and SEM), chemical composition (XPS), optical properties (Spectroscopic Ellipsometry and UV-VIS Spectroscopy) and electrical properties (Hall Effect) in comparison with undoped Cu_2O films. The obtained films are adherent and uniform with a thickness in the range of 170-200 nm and exhibit optical transparency of over 80% in the VIS-NIR domain. Besides XPS, the presence of Sr in the films matrix was evidenced by Raman Spectroscopy and Infrared Ellipsometry. Hall Effect measurements emphasized the p-type electrical conductivity of the Cu_2O-Sr films, with carrier concentration in the range of 10^{16}-10^{17} cm^{-3}. The optical constants of the Cu_2O-Sr films were obtained over a wide wavelengths range.

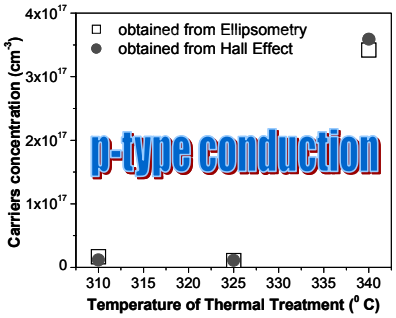

INTRODUCTION

Nowadays the advanced optoelectronic applications (smart windows, panels, solar cells, etc) requires new transparent and p-type conductive materials, given that the most used transparent conductive oxides (TCO) exhibit n-type conductivity, with Indium Tin Oxide (ITO) being the most popular among them. In this respect, preferably would be to obtain a transparent (T>75%) and conductive (N>10^{16} cm^{-3}) material, with band gap energy (Eg) greater than 3 eV and a tunable conductivity by using specific dopants. One example of such a material currently studied as ITO replacement is zinc oxide (ZnO), which has a n-type conductivity. By using certain methods (for example co-doping with In and N) it can be changed into a material with stable p-type conductivity.[1] Under these circumstances, based on literature theoretical predictions,[2] we propose in this work the obtaining of Sr doped Cu_2O (Cu_2O-Sr) films as p-type TCO material. Undoped Cu_2O has band gap energy of 2.1 eV and p-type conductivity.[3] The presence of Sr inside Cu_2O matrix leads to increase in the band gap energy by interrupting Cu-Cu type network interactions.[4]

* Corresponding author: manastasescu@icf.ro and mnicolescu@icf.ro; Tel: +40213167912; Fax: +40213121147

** This work is meant to be part of the special volume of Revue Roumaine de Chimie honoring Academician Maria Zaharescu and her major contributions towards the development of sol-gel materials chemistry

It is worth to mention that the preparation of Cu_2O-Sr films on the basis of the sol-gel method is complicated by the presence of the unavoidable strontium carbonate, while the obtaining of the same material by sputtering technique is hampered by the lack of proper commercial targets. Therefore, MOCVD was used in this work in order to obtain a new class of materials with good optoelectronic properties based on Sr-doped Cu_2O films (Cu_2O-Sr).

RESULTS AND DISCUSSION

1. Structural characterization

1.1. XRD

The X-ray diffractograms of the prepared films are shown in Fig. 1. Based on XRD analysis, the crystal structure of the CUP 08 and CUP 09 thin films samples was assigned to cubic Cu_2O, according to the ICDD file no. 00-005-0667. By Sr doping of Cu_2O, the tetragonal phase of $SrCu_2O_2$ could not be stabilized or could not be identified within the detection limits of the instrument. The unit cell parameters were a=b=c=4.2869(5) Å for CUP 09 sample and, respectively, a=b=c=4.2864(5) Å for sample CUP 08. The unit cell parameters were larger than the values reported in the ICDD file (where a=b=c=4.2696 Å). This increase could be influenced by the nature of the substrate. It also can be noticed that the position of Bragg reflection with Miller indices (200) is slightly displaced to lower 2θ value (larger d-spacing). The crystallite size was 106.39(10) Å for CUP 09 sample and, respectively 145.2(3) Å for CUP 08 sample.

Sample CUP 20 contains, besides the Cu_2O crystalline phase, a second crystalline phase (marked with an asterisk in the Fig. 1), identified as SrF_2 (ICDD file no. 86-2418), which are contaminants from deposition chamber and an amorphous phase due to substrate or unreacted reagents. A third crystalline phase, marked with # in the Fig. 1, remains unidentified as long as its reflection cannot be assigned to any of Sr or Cu based compounds or to the substrate. The unit cell parameters of Cu_2O crystal phase were a=b=c=4.254(2) Å for CUP 20 sample, with a crystallite size of 118.4(2) Å.

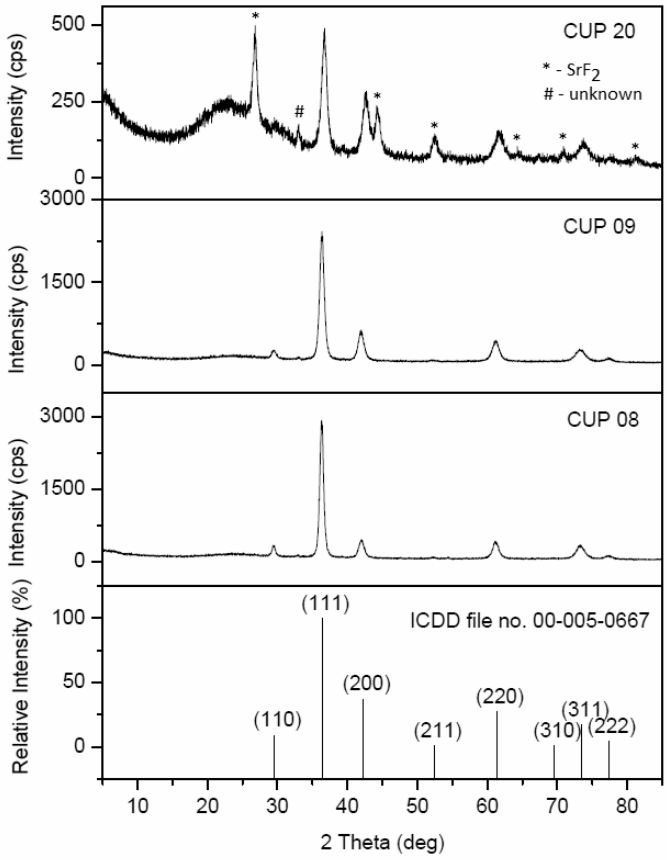

Fig. 1 – X-ray diffractograms of the Sr doped Cu_2O films compared with Cu_2O pattern (ICDD file no. 00-005-0667).

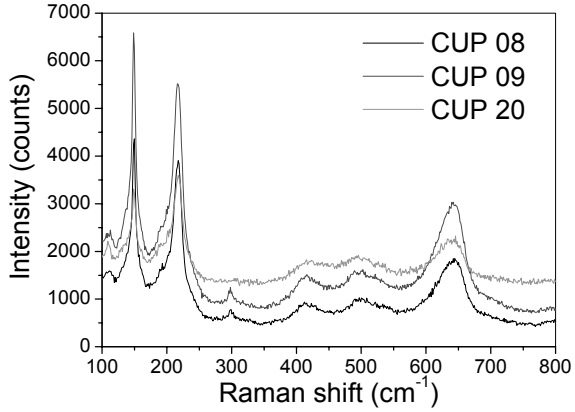

Fig. 2 – Raman spectra of the films.

Table 1

Raman vibration assignation

Literature [5-8] vibration data (cm^{-1})	**CUP samples vibration data (cm^{-1})**	**Assignation**
144, 215, 409, 623	148, 218, 414, 644	Cu_2O
285	299	SrF_2
444, 454, 502	495	SiO
524	–	$SrCu_2O_2$

1.2. Raman spectroscopy

The Raman spectra were measured with a InviaReflex Renishaw MicroRaman using the 514 nm laser excitation. The laser power was kept under 2mW in order to avoid any heating effects. The Raman spectra of the films are depicted in Fig. 2, while the assignations of the vibration modes are summarized in Table 1. Noteworthy that $SrCu_2O_2$ band which should appear at 520–530 cm^{-1} is missing, thus $SrCu_2O_2$ tetragonal phase didn't form, which confirm the XRD results.

2. Morphological characterization

2.1. AFM

Atomic force microscopy measurements have been performed in order to evaluate the morphology and the roughness of the CUP samples. Fig. 3 shows the topographic AFM images at the scale of (8 x 8)μm^2, together with characteristic surface profiles collected along the fast scanning direction.

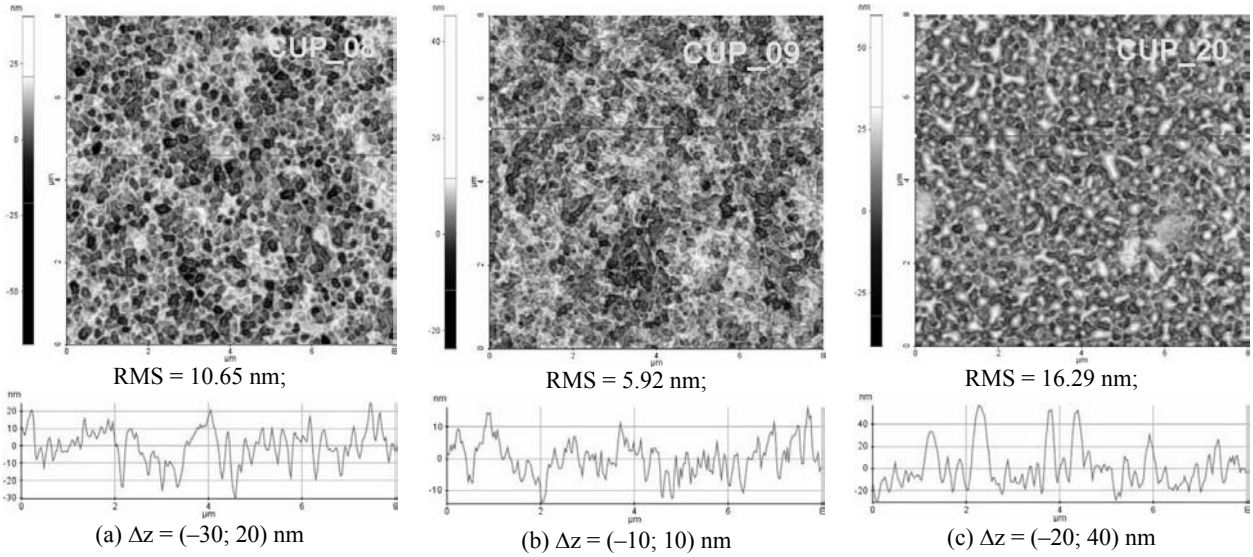

RMS = 10.65 nm; RMS = 5.92 nm; RMS = 16.29 nm;

(a) $\Delta z = (-30; 20)$ nm (b) $\Delta z = (-10; 10)$ nm (c) $\Delta z = (-20; 40)$ nm

Fig. 3 – Two-dimensional characteristic AFM images together with arbitrary surface profiles (line scans).

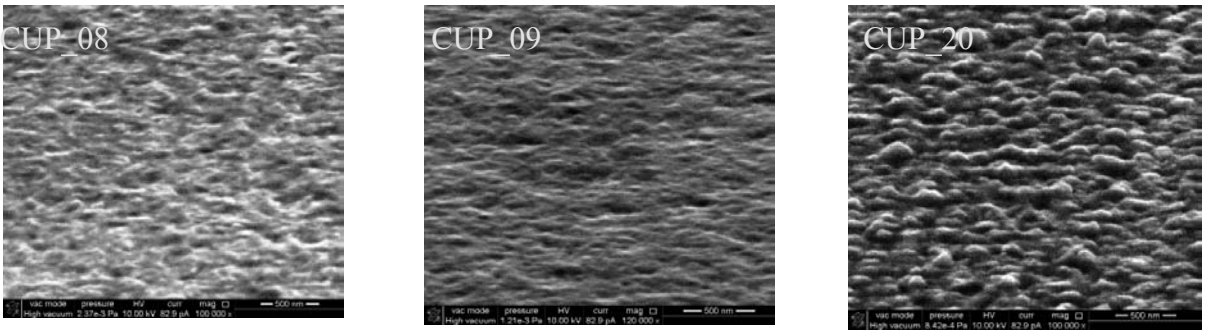

Fig. 4 – SEM images of Cu_2O-Sr films.

The presence of Sr in the Cu_2O matrix (in a ratio Sr:Cu of 3:1 – sample CUP 08) leads to well defined surface morphology consisting in a homogeneous distribution of superficial pores, with diameters of up to 100 nm and 20–30 nm in depth (Fig. 3a). The Sr-free sample (CUP 09) shows the smoothest surface, with peak-to-valley distance of about 20 nm, as could be observed from the corresponding surface line-scan (Fig. 3b). Accordingly the roughness increases to about 11 nm. But then, the sample with Sr:Cu ratio of 1:1 (CUP 20) have a different morphology, consisting in rounded hills with heights up to 40 nm, leading to the largest roughness value in the sample series, close to 16 nm and peak-to-valley distance of about 60 nm (Fig. 3c).

2.2. SEM

High resolution SEM images of the Cu_2O-Sr film surfaces are presented in Fig. 4. It can be seen, consistent with AFM analysis, the formation of continuous, homogeneous and substrate adherent films, with larger particles present on the CUP 20 sample surface only.

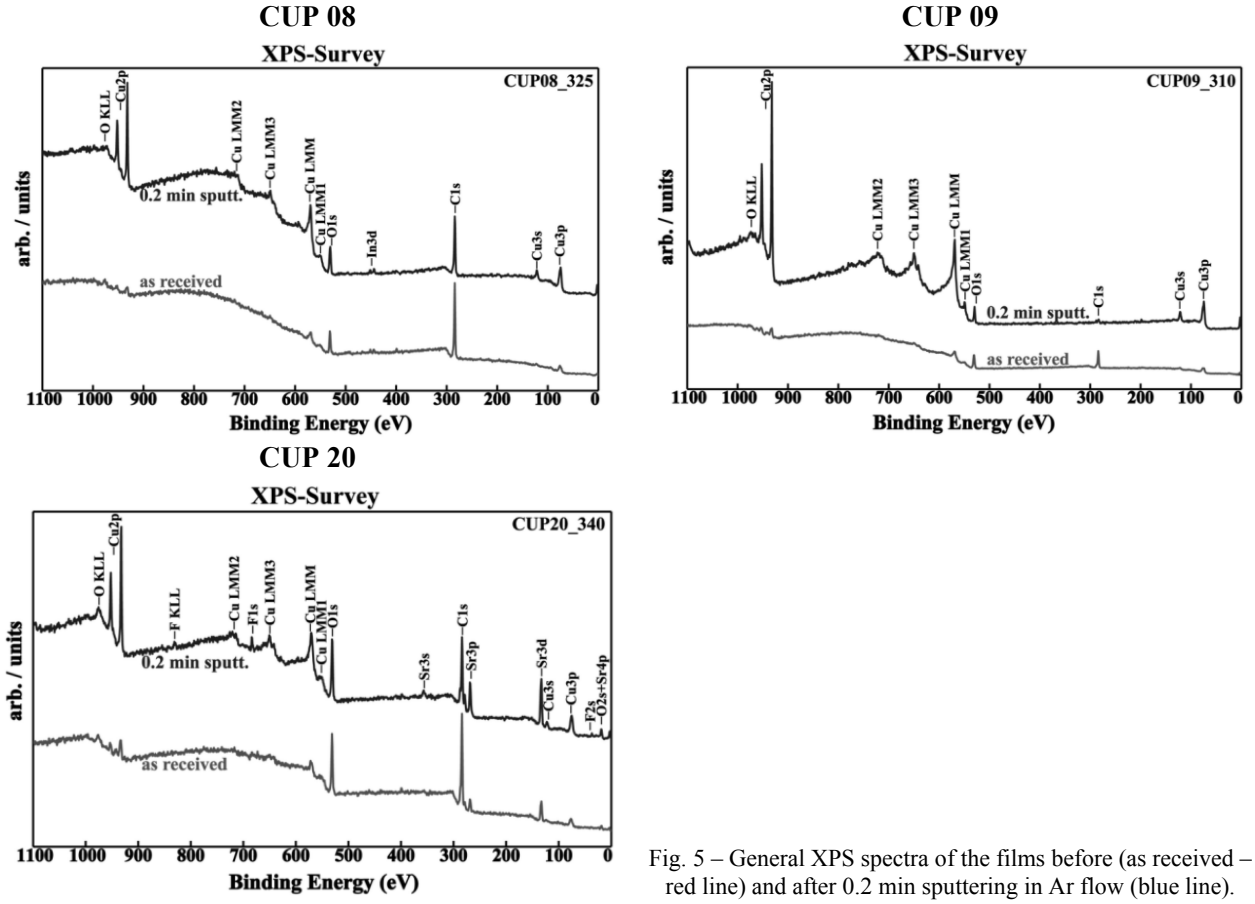

Fig. 5 – General XPS spectra of the films before (as received – red line) and after 0.2 min sputtering in Ar flow (blue line).

3. Chemical characterization (XPS)

XPS analysis was used to determine the chemical states of the elements present on the surface and their relative concentrations. There were recorded general spectra (Fig. 5) and high resolution spectra (Fig. 6) of the most significant XPS transitions (C1s, O1s, F1s, Cu2p and Sr3d) for the CUP samples with an error of ±5.0% for quantitative analysis and ± 0.2 eV in assigning the binding energies (BE).

From the high resolution Sr3d spectra (Fig. 6) Sr was observed on the surface of the sample CUP 20, and the fact that there is no signal for the other samples, leads to the idea that Sr is located below the analyzed area, possibly migrating to the "bulk" area. Due to surface contamination with a large amount of carbon (Table 2), the XPS signal was recorded before and after Ar ion sputtering, in order to determine the chemical species of the surface and of the region below the surface.

From the relative concentrations of the elements in the analyzed samples and the deconvolution of the spectra it can be concluded that C is present in a significant percentage on the surface, as a residue of the organometallic compounds used.

Cu it partially oxidizes and remains in the metallic state in the absence of oxygen. One important aspect is related to the existence of only monovalent Cu. Copper does not exist in its divalent state in the samples (CuO exhibits very low transparency). This result explains the better quality in terms of the transparency for the studied MOCVD films. The Sr ions present on the surface is more reactive than Cu, reacting rapidly with C and forming $SrCO_3$. It was also detected the presence of F-traces (from the deposition chamber) that fluorinate Sr but mainly binds to C, forming bonds of the CF_n type.

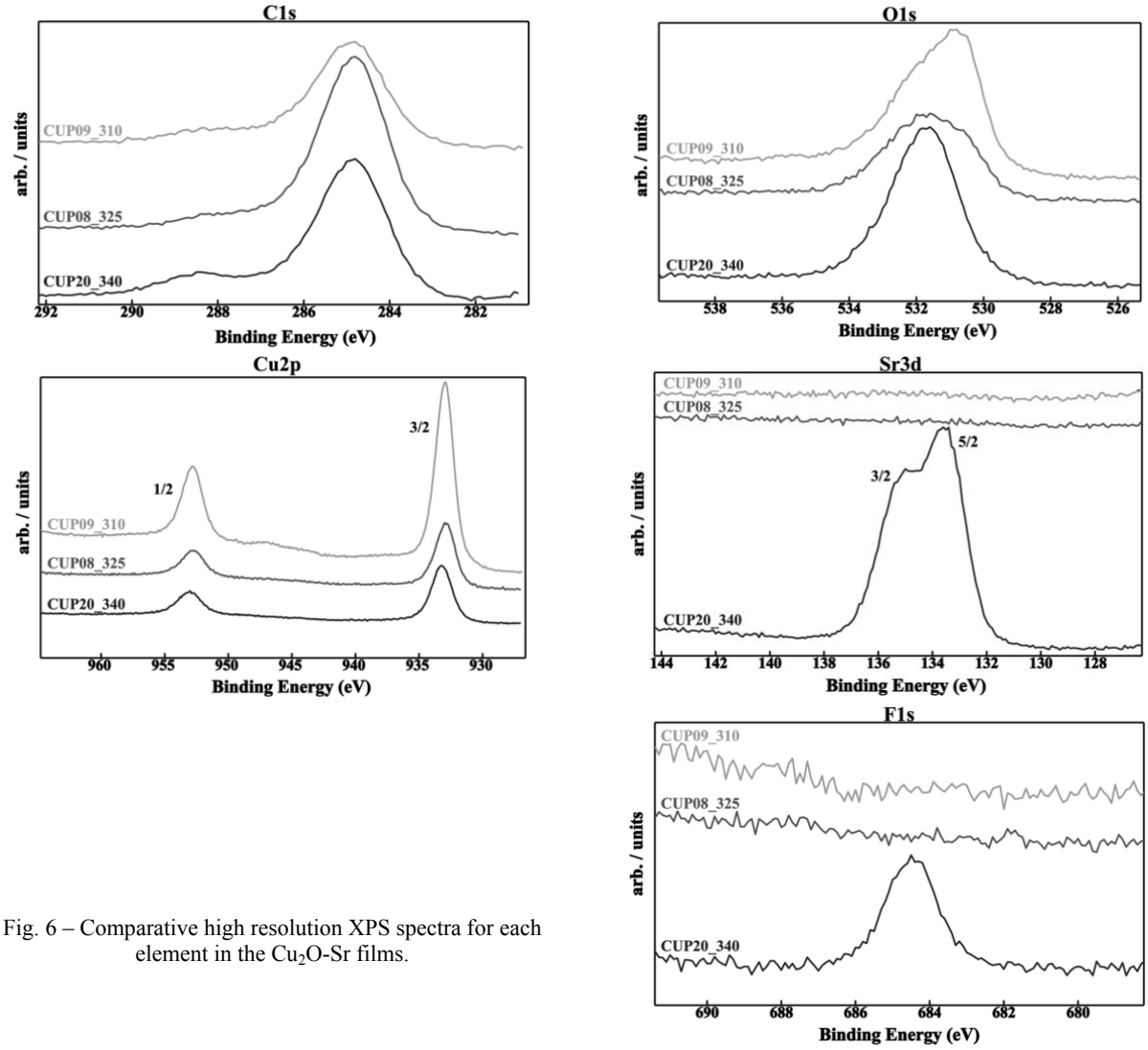

Fig. 6 – Comparative high resolution XPS spectra for each element in the Cu_2O-Sr films.

Table 2

Relative concentrations of elements (% at) on the films surface (~10nm)

Sample	C1s	O1s	Cu2p	Sr3d	F1s
CUP 08	76.7	16.2	7.1	–	-
CUP 09	52.5	27.8	19.7	–	-
CUP 20	61.5	22.7	6.0	6.8	3.0

Table 3

Film thickness (d_{film}), roughness layer ($d_{roughess}$) and the value of the optical band gap (Eg)

Sample	d_{film} (nm)	$d_{roughess}$ (nm)	E_g (eV)
CUP 08	193.4	18.7	3.00
CUP 09	179.7	11.4	2.72
CUP 20	96.4	50.6	2.75

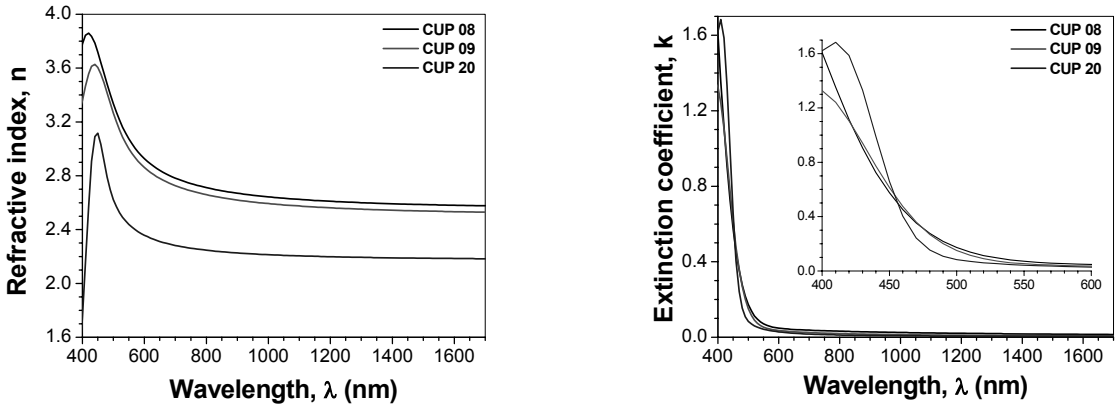

Fig. 7 – Dispersion of the refractive index (n) and absorption coefficient (k) of the Cu_2O-Sr films in the VIS-NIR spectral range.

4. Optical characterization

4.1. Spectroscopic Ellipsometry (SE) in VIS-NIR domain

The optical properties of the Cu_2O-Sr films have been investigated by the spectroscopic ellipsometry firstly in the VIS – NIR spectral range (400-1700 nm). The layer thicknesses, the optical constants (refractive index -n and extinction coefficient - k) and the band gap energy have been obtained by fitting of the experimental data. Thus, the analysis of experimental Psi and Delta spectra was performed with a three-layer model: substrate/film/roughness using mathematical models (functions) containing Gauss-Lorentz and Drude oscillators. To model the roughness layer, which is considered a mixture of 50% material (film) and 50% voids (air), the Bruggemann's effective medium approximation (B-EMA) was used[9]. The thickness of the layer, the energy, and respectively the amplitude and the width of the oscillators have been employed as fitting parameters. The obtained ellipsometric results are summarized in Table 3.

Based on the ellipsometric results, a decrease in the refractive index is observed (Fig. 7) depending on the applied thermal treatment, which can be due to both the presence of surface defects highlighted by the AFM and the carbonate presence in the composition of the films, as evidenced XPS and by IR-SE as will be shown in section 4.2.

As it can be seen, the value of the optical band gap (Table 3) increases with the amount of Sr introduced in the films matix, which will lead to a significant improvement in electrical properties (see below).

Based on the ellipsometric analysis, the dielectric function of the Cu_2O-Sr films was obtained, by combining the Gauss-Lorentz (GL) model (describing the absorption in the UV range caused by the dopant's high concentration) with the Drude (D) model (describing the effect of the electric charge carriers on the dielectric function when passing from the visible to the infrared wavelength range). Thus, the total dielectric function is given by the following equation:

$$\varepsilon(E) = \varepsilon_r + i\varepsilon_i = \varepsilon_{G\text{-}L} + \varepsilon_D, \quad (1)$$

where ε_r is the real part and ε_i is the imaginary part of the dielectric function, respectively the dielectric contribution of the Gauss-Lorentz (ε_{G-L}) and Drude (ε_D) models. At low energies (E <1.5eV, λ> 800 nm) the real part of the dielectric function ε_{G-L} is given by the dielectric constant at the high-frequency ε_∞. Under these conditions, the total dielectric function can be written as:

$$\varepsilon(E) = \varepsilon_\infty + \varepsilon_D, \text{ where } \varepsilon_D = -\frac{A_D}{E^2 + iB_D E}, \quad (2)$$

The Drude oscillator contains two terms: the amplitude (A_D), which is proportional to the carriers, respectively the plasma frequency and the second term, namely the scattering frequency (B_D), given by the equations[10]:

$$A_D = \varepsilon_\infty E^2{}_p = \hbar^2\omega_p^2,\ B_D = \hbar\gamma,\ \omega_p = \frac{2\pi c}{\lambda_{\min}}\sqrt{\frac{\varepsilon_\infty - 1}{\varepsilon_\infty}},\ \omega_p^2 = \frac{Nq^2}{\varepsilon_0 m^*(\varepsilon_\infty - 1)} - \gamma^2, \quad (3)$$

Thus, the carriers concentration, the mobility and the optical conductivity were determined using the Drude model from SE data, described by the equations:

$$\rho = \frac{\gamma}{\varepsilon_0\omega_p^2} \rightarrow \rho = \frac{m^*}{Nq^2\tau} = \frac{1}{q\mu N},\ \sigma = en\mu = 1/\rho, \quad (4)$$

Table 4 shows the electrical parameters obtained from the ellipsometric analysis. The validity of the ellipsometric analysis was confirmed by a good agreement between the values of the carriers concentration, mobility, resistivity and conductivity with those determined from Hall effect measurements (Fig. 8).

Table 4

Electrical parameters obtained from SE for the Cu_2O-Sr samples

Sample	Rezistivity (Ωcm)	Charge carriers concentration (cm^{-3})	Mobility (cm^2/Vs)	Conductivity (S/cm)
CUP 08	1.0515×10^2	1.0871×10^{16}	5.4606	9.510×10^{-3}
CUP 09	6.310×10	1.6875×10^{16}	5.8708	1.058×10^{-2}
CUP 20	12.41×10	3.4207×10^{17}	1.4703	8.058×10^{-2}

4.2. Infrared ellipsometry (IR-SE)

The optical model used in the VIS-NIR spectral range was extended in Infrared wavelengths domain in order to fit the experimental Ψ and Δ spectra. IR-SE which combines the advantages of ellipsometry and of the infrared spectroscopy was used not only to extend the optical constants of the Cu_2O-Sr films in the IR domain but also to asses the characteristic chemical bonds of the analyzed samples. Thus, the assignation of the characteristic vibrational bands of the components was done from the dielectric loss function (Fig. 9 and Table 5). Bands related to the vibration of oxygen in the Cu-O and Sr-O bonds were identified (Table 5), proving the incorporation of the dopants in the matrix of the films. The presence of the Sr-O ($SrCO_3$) vibration bonds, observed in IRSE analysis confirms the XPS results (Table 2). The optical constants extended in the IR range are presented in Fig. 10.

4.3. UV-VIS spectroscopy

In order to evaluate the transmission, a property which is absolutely necessary for the practical application of TCO materials, the Cu_2O-Sr films were measured by UV-VIS spectrophotometry in the 250-2500 nm wavelengths range, the results being shown in Fig. 11.

It can be seen that the analyzed films have a transparency over 80%, favorable to the TCO applications, the maximum transmission function being obtained for the CUP 20 sample, corresponding to a Sr:Cu ratio of 1:1.

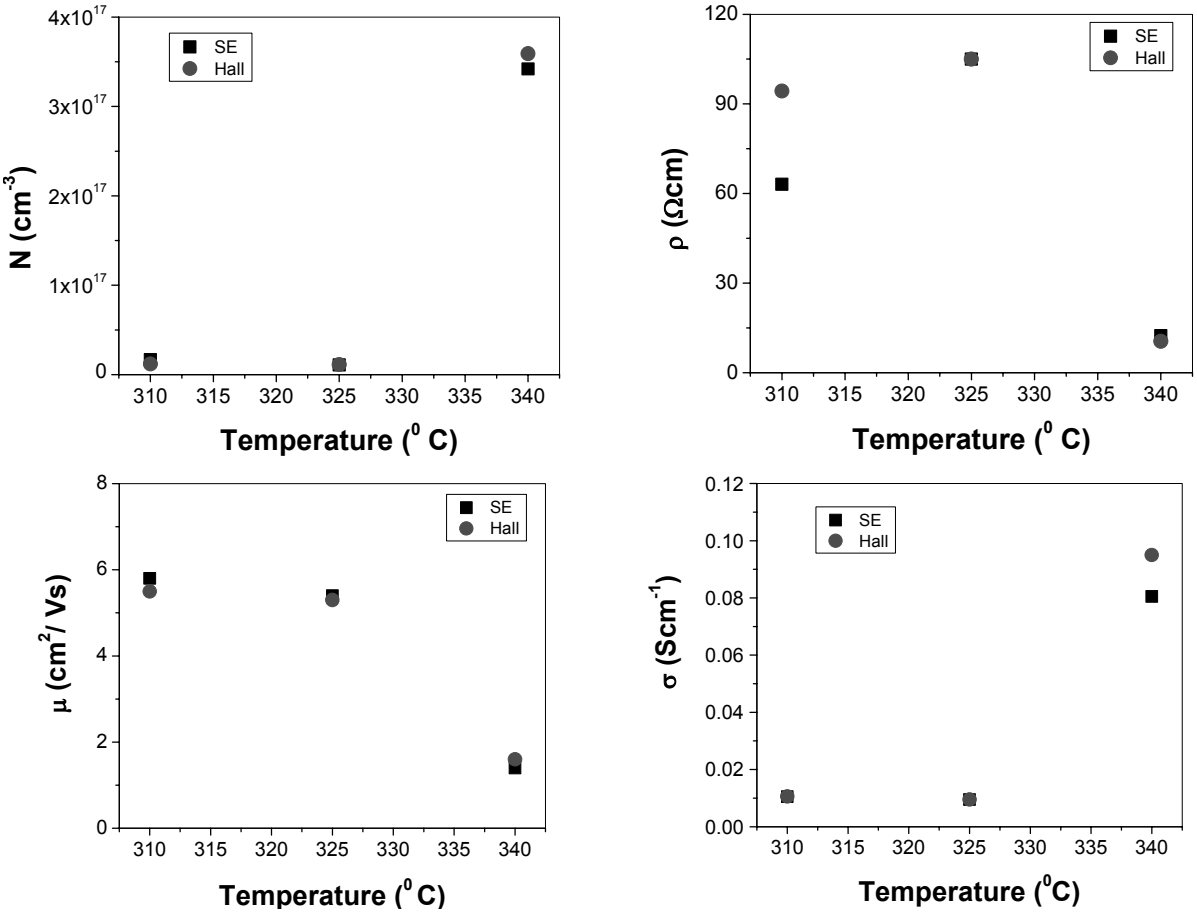

Fig. 8 – Comparison of the electrical parameters as obtained by SE and Hall methods.

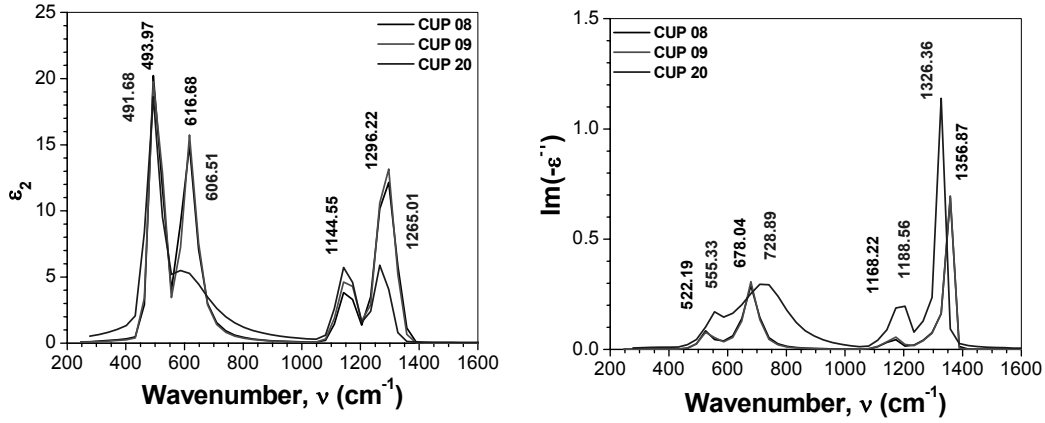

Fig. 9 – The imaginary part of dielectric function (ε_2) and dielectric loss function (Im-e^{-1}) of Cu_2O-Sr films.

Table 5

IRSE vibration assignation

Literature[8,11,12] phonon frequencies (cm^{-1})	Optical phonon frequencies (cm^{-1})		Assignation
	ω_{TO}	ω_{LO}	
497, 524, 529, 557	493.53	556.76	$SrCu_2O_2$
608.2, 615, 626.5	605.43	725.33	Cu_2O
1144	1144.29	1188.56	$SrCO_3$
	1265.34	1326.36	-

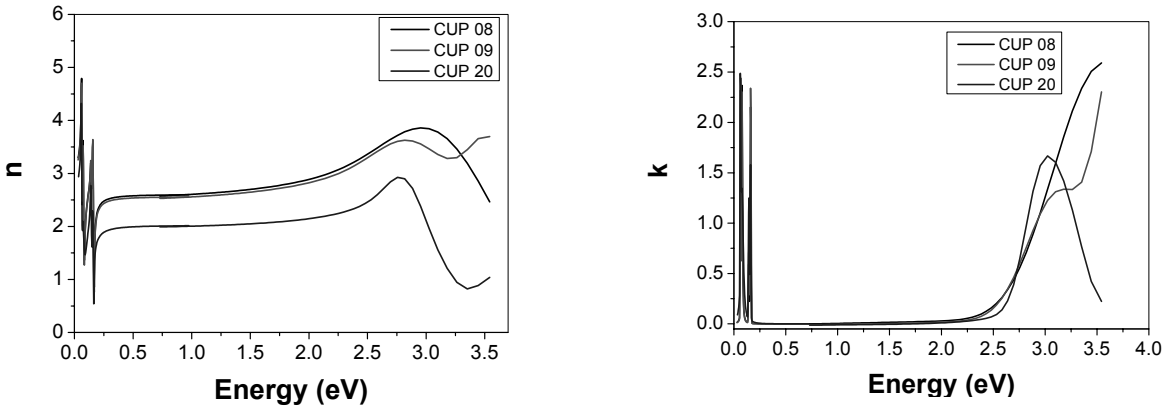

Fig. 10 – Dispersion of the refractive index (n) and absorption coefficient (k) of the Cu_2O-Sr films over a wide spectral range (0.7-3.5eV).

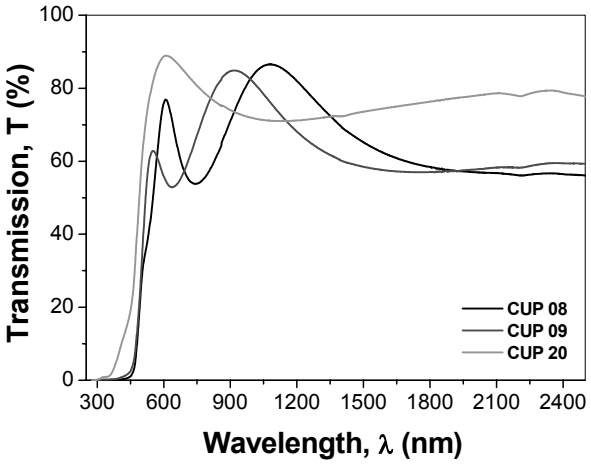

Fig. 11 – UV-VIS-NIR transmission spectra of the Cu_2O-Sr films.

Table 6

Electrical parameters of the Cu_2O-Sr films

Sample	Conduction type	N_A (cm^{-3})	ρ (Ωcm)	μ (cm^2/Vs)
CUP 08	P	1.12×10^{16}	1.05×10^{2}	5.3
CUP 09	P	1.20×10^{16}	9.43 x 10	5.5
CUP 20	P	3.59×10^{17}	1.05 x 10	1.6

5. Electrical characterization

The main electrical parameters: carrier concentration (N_A), mobility (μ) and resistivity (ρ), as determined from Hall Effect measurements, are presented in Table 6.

As it can be observed, both doped oxides exhibit p-type conduction, with different performance. The high resistivity (in the range of 10–100 Ωcm), as well as the relatively low carrier concentration (10^{16} – 10^{17} cm^{-3}) would suggest that the positive charges are trapped at some defect sites that act as electron donors in the film. The fact that the highest carrier concentration is obtained for the CUP 20 sample, would suggest that this meets two advantages:

- the doping level/concentration/ratio is high enough to promote an increase in holes in the film compared to the pristine Cu_2O and
- the doping level/concentration/ratio is low enough to not introduce defects in the lattice and thus trigger charge trapping or scattering, which would increase resistivity (see CUP 08).

As determined from the structural analysis, the introduction of Sr could not stabilize the tetragonal

phase of $SrCu_2O_2$, but it has led to a significant increase in band gap energy and in the carrier concentration, compared to the pure copper oxide.

EXPERIMENTAL

1. Thin film deposition

Cu_2O-Sr films were deposited by Metal Organic Chemical Vapor Deposition (MOCVD) method on Corning 1737 glass. Copper bis(2,2,6,6-tetramethyl-3,5-heptanedionate) from Sigma ALDRICH and Strontium bis(2,2,6,6-tetramethyl-3,5-heptanedionate) dehydrate from STREAM Chemicals were used as precursor for Cu and Sr, respectively. The composition and deposition temperature of the films are given in Table 7. Two different Sr:Cu ratios have been prepared in comparison with pristine Cu_2O prepared in the same experimental setup (device).

Table 7

Cu_2O-Sr films obtained by MOCVD

Sample	Molar ratio Sr:Cu	TT* (°C)
CUP 08	3:1	325
CUP 09	0:1**	310
CUP 20	1:1	340

* TT = temperature of thermal treatment;
** CUP 09 = reference sample, containing only Cu_2O

2. Thin films characterization

X-Ray Diffraction (XRD) patterns were recorded using a Rigaku Ultima IV multifunctional diffraction system. The equipment was set in asymmetric diffraction geometry (*"thin films method"*), with parallel beam (PB) optics. The diffractometer was operated at 40 kV and 30 mA, using Cu Kα (λ = 1.5406 Å) radiation. The instrument was operated in continuous scan mode, with a scan speed of 1°/min and a step-width of 0.02° (2θ), at a fixed incident angle, α, of 0.5°. Data were collected over the 2θ range from 5 to 85°. The crystalline phase identification was done by PDXL software connected to the ICDD PDF-2 database.

Raman Spectroscopy measurements were carried out using an InviaReflex Renishaw using a 514 nm laser excitation.

Atomic Force Microscopy (AFM) measurements were carried in non-contact mode, with XE-100 apparatus from Park Systems, using sharp tips (< 8 nm tip radius; PPP-NCHR type from Nanosensors™), at the scale of (8x8) μm^2. The XEI (V.1.8.0) Image Processing Program developed by Park Systems was used for displaying purpose and subsequent data analysis, including the calculation of the root mean square (RMS) roughness. In order to have a better view of the surface morphology, the AFM images are presented in the paper in so-called "enhanced color"™ view mode, which uses the change of pixel relative to its neighbors.

Systematic information on the thin film morphology has been obtained by **scanning electron microscopy (SEM)** analysis using a FEI Quanta 3D microscope operating between 5 and 30 kV, coupled with energy dispersive X-ray spectroscopy (EDX) measurements.

The **XPS** measurements were carried out on PHI Quantera equipment at a residual pressure of 10^{-7} Pa in the analysis chamber. The X-ray source was monochromatized Al K_α radiation (1486.6 eV) and the overall energy resolution is estimated at 0.65 eV by the full width at half maximum (FWHM) of the Au4f7/2 line. The XPS spectra were calibrated using the C1s line (binding energy, BE = 284.8 eV) of the adsorbed hydrocarbon on the sample surface (C–C or (CH)n bondings) and the charging effect was minimized by using dual beams (electrons and Ar ions) as neutralizer. The errors in our quantitative analysis (relative concentrations) were estimated in the range of ±10%, while the accuracy for binding energy assignments was ±0.2 eV.

The **spectroscopic ellipsometry (SE)** measurements were performed on J.A. Woollam Co. ellipsometer in two separate spectral regions, i.e., in Vis-NIR (0.4-1.7 μm) and IR (2-30 μm) spectral range. The IR-SE measurements were performed at 60 and 70° angle of incidence, $64cm^{-1}$ resolution and 100 scan/spectrum. WASE program from Woollam was used for multi-parameter fitting program in which an iterative least-squares method is used for minimizing the difference (mean square error - MSE) between the experimental theoretical data.

UV-VIS spectrophotometry measurements have been performed in normal incidence configuration using a double spectrophometer Perkin Elmer Lambda 950 using a resolution of 1nm.

Hall Effect measurements have been performed with HMS-500 Ecopia instrument (van der Pauw method).

CONCLUSIONS

A new class of TCO materials with p-type conductivity was obtained by MOCVD method based on strontium-doped copper oxide. Films with 3:1 and 1:1 Sr:Cu molar ratios in comparison with pristine Cu_2O have been investigated by a combination of characterization methods in relation to their structural, chemical, morphological and optoelectronic properties.

The MOCVD films are adherent and uniform with a thickness in the range of 170-200 nm. XPS highlighted the presence of monovalent and the absence of bivalent copper.

The strontium-doped copper oxide films obtained by MOCVD show a transparency higher than 80% and a holes concentration of 10^{16}-10^{17} cm^{-3}, which recommends them as p-type TCO materials suitable for optoelectronic and photovoltaic applications.

Acknowledgements: This work was supported by the project "Sustainable autonomous system for nitrites/nitrates and heavy metals monitoring of natural water sources" - M-ERA.net 39/04.01.2016. Support of the EU (ERDF) and Roumanian Government that allowed for acquisition of the research infrastructure under POS-CCE O 2.2.1 project INFRANANOCHEM – No. 19/01.03.2009, is gratefully acknowledged.

REFERENCES

1. M. Duta, S. Mihaiu, C. Munteanu, M. Anastasescu, P. Osiceanu, A. Marin, S. Preda, M. Nicolescu, M.

Modreanu, M. Zaharescu and M. Gartner, *Appl. Surf. Sci.*, **2015**, *344*, 196-204.
2. M. Nolan and S.D. Elliott, *Phys. Chem. Chem. Phys*., **2006**, *8*, 5350-5358.
3. K. Tonooka, K. Shimokawa and O. Nishimura, *Thin Solid Films*, **2002**, *411***,** 129-133.
4. Y. Nakano, S. Saeki and T. Morikawa, *Appl. Phys. Lett.*, **2009**, *94*, 022111-1_022111-3.
5. Ł. Ciupiński, E. Fortuna-Zaleśna, H. Garbacz, A. Koss, K. J. Kurzydłowski, J. Marczak, J. Mróz, T. Onyszczuk, A. Rycyk, A. Sarzyński, W. Skrzeczanowski, M. Strzelec, A. Zatorska and G. Z. Żukowska, *Sensors*, **2010**, *10*, 4926-4949.
6. A.V.R. Warrier and R.S. Krishnan, *Naturwissenschaften*, **1964**, *51*, 8-9.
7. T.P. Nguyen and S. Lefrant, *Solid State Comm.*, **1986**, *57*, 235-236.
8. J. Even, L. Pedesseau, O. Durand, M. Modreanu, G. Huyberechts, B. Servet and O. Chaix-Pluchery, *Thin Solid Films*, **2013**, *541*, 113-116.
9. D.E. Aspnes, J.B. Theeten and F. Hottier, *Phys. Rev. B*, **1979**, *20*, 3292-3302.
10. H. G. Tompkins, WVASE32 Software Training Manual for IR-VASE, J.A.Woollam CO. Inc., Lincoln, NE, USA, **2006**.
11. J. L. Deschanvres, C. Millon, C. Jimenez, A. Khan, H. Roussel, B. Sevet, O. Durand and M. Modreanu, *Phys. Stat. Sol. (A)*, **2008**, *205*, 2013-2017.
12. G. Papadimitropoulos, N. Vourdas, V. Em. Vamvakas and D. Davazoglou, *J. Phy. Conf. Series*, **2005**, *10*,182–185.